Room-temperature large edge-magnetism in oxidized few-layer black phosphorus nanomeshes

Y. Nakanishi[1], D. Soriano[3], C. Ohata[1], R. Iwaki[1], Y. Katagiri[1], Y. Fukai[1], K. Nomura[1], T. Nakamura[2], S. Katsumoto[2],

S. Roche[3,4], J. Haruyama[1]

[1] *Faculty of Science and Engineering, Aoyama Gakuin University, 5-10-1 Fuchinobe, Sagamihara, Kanagawa 252-5258, Japan*
[2] *Institute for Solid State Physics, The University of Tokyo, 5-1-5 Kashiwanoha, Kashiwa, Chiba277-8581, Japan*
[3] *ICN2-Institut Catala de Nanociencia i Nanotecnologia, Campus UAB, 08193 Bellaterra (Barcelona), Spain*
[4] *Institució Catalana de Recerca i Estudis Avançats (ICREA), Barcelona, 08070, Spain*

The formation of edge magnetism in two-dimensional (2D) materials has been only experimentally observed in hydrogenated graphene nanoribbons and graphene nanomeshes (GNM). The measured magnetization values of these systems are, however, also far too small to allow envisioning practical applications. Herein, we report the experimental observation of room-temperature large edge ferromagnetism in oxidized few-layer black phosphorus nanomeshes (BPNMs). The values of the observed robust edge magnetism per single pore are ~100 times larger than that reported for hydrogenated GNMs, whereas the magnetism disappears in hydrogenated BPNMs. The ferromagnetic coupling of edge P atom with O atom and the strong spin localization of edge valence band can be the origins as well as uniform oxidation of pore edges and interlayer edge interaction. Such finding paves the way for realizing high-efficiency 2D flexible magnetic and spintronic devices without the use of rare magnetic elements as atomic layers replacing graphene.

The zigzag-type atomic structure of graphene edges leads to spin polarization and flat-band ferromagnetism (FM) from theoretical viewpoints[1-4]. From experimental respect, flat-band FM has been realized based on the fabrication of hydrogen (H)-terminated zigzag-edged GNMs consisting of a honeycomb-like array of hexagonal nano-pores (similar to Fig. 1E), fabricated using a non-lithographic method, resulting in low-disordered and low-contaminated pore edges[5-12]. Because a GNM corresponds to a large ensemble of zigzag-edged graphene nanoribbons (GNRs), it is effective to detect small magnetic signals arising from the pore edge spins. Nevertheless, the observed magnetization values so far have been as small as $\sim 10^{-6}$ emu/100 μm^2, [6,7] except for some specific case[8].

Mono- or few-layer black phosphorus (BP) appears as a high-mobility 2D semiconductor with a substantial energy band gap[13,14]. BP has a puckered honeycomb lattice, easily oxidized under air atmosphere exposure, with an in-plane anisotropic atomic structure (Fig. 1A) [13-25]. Regarding those magnetism, only theoretical works have been reported up to now[17,18,21]. In particular, spin polarization arising from edge dangling bonds has been predicted in pristine zigzag-edged phosphorene NRs (ZPNRs)[17]. Oxygen (O)-saturated zigzag PNRs show edge FM due to the spins of unsaturated bonds in weak P–O bonds along the p_z orbitals in the NR plane, whereas H-terminated zigzag PNRs show no edge FM. This behavior highly contrasts with that of GNMs[6]. Moreover, even stronger and highly stable edge anti-ferromagnetism (AFM) has been predicted in ZPNRs due to the electronic instability induced by the half-filled 1D bands[21].

In the present experiments, flakes of few-layered BPs were mechanically exfoliated from bulk BP (Smart Element Co.) using the Scotch tape method and observed via optical microscope (Fig. 1C) and atomic force microscope (Fig. 1D). Following application of a non-lithographic method[12] (Supplementary Material (SM) 1-5), few-layer BPNMs were fabricated (Fig.1E). Interpore regions correspond to BPNRs, but only two edges of each hexagonal pore can be simultaneously perfect zigzag shaped because of the topological reason that the inner angle of the puckered honeycomb lattice ~98.15° (Fig. 1B) cannot be aligned to the inner angle of the hexagonal pore of 120°. This is different from the case of GNM. The samples were annealed at a critical temperature (T_c) of ~300 °C in a high vacuum (~10^{-6} torr) (SM 6)[26]. Absence of substantial background magnetic impurities and magnetic contamination has been also confirmed by Electron Energy Loss Spectroscopyand Micro-Auger Electron Spectroscopy in four samples. Subsequently, each sample was placed in an air atmosphere at 300 K for 2 h, resulting in O-termination of pore edges[23]. Immediately following this annealing process, magnetization was measured using superconducting quantum interference devices (Quantum Design Co.).

Figure 2A shows measurement results of the magnetization of the O-terminated BPNM. Ferromagnetic (FMC)-hysteresis loops are observed with $M_s \sim 10^{-4}$ emu/100 μm^2. Importantly, the hysteresis loop at T = 2 K approximately remains as it is

even at T = 300 K. On the other hand, the few-layer bulk BP flakes with all the same fabrication process as those for Fig. 2A-sample but forming no pore (Fig. 2B) and just with Ar gas etching process without using porous alumina template mask (but with the same condition as that for pore forming) (inset of Fig. 2B) showed no magnetization. This important result indirectly reconfirms that the FM observed in Fig. 2A originates solely from the formation of oxidized nano-pores. This no magnetism has been confirmed at least in three samples. Indeed, observation of this FMC-BPNM by magnetic force microscope shows presence of polarized spins around pore edges (inset of Fig. 2A).

Since the oxidation of pore edges is easily obtained by exposing BPNM into air atmosphere, one can assume that all pores in a BPNM are O-terminated and can become magnetic. With such an assumption, the magnetic moment per single pore area (μ_{pore}) is estimated to be ($\sim 0.5 \times 10^{-12}$)/ ($\mu_B = 9.3 \times 10^{-24}$) $\sim 5 \times 10^{10}$ μ_B, where μ_B is the Bohr magneton[29]. Following ref. 6, μ_{pore} of partially ($\sim 10\%$) H-terminated FMC-GNM annealed under H_2 atmosphere was estimated to be $\sim 5 \times 10^8$ μ_B. Therefore, μ_{pore} of the O-terminated BPNM is approximately 100-times larger than that in the H-terminated GNM[6,7]. Accordingly, BP has a significant advantage in which O-terminate edge generate room-temperature magnetism, in contrast with the much smaller magnetism obtained by partially H-terminated edges in GNM.

Figure 2C reveals that the non-annealed BPNM demonstrates a FMC hysteresis loop with a M_s value ~ 4 times less than those of the T_c-annealed samples (i.e., Fig. 2A). This result implies that annealing at the T_c is important for introducing large FM. Indeed, reproducibility of magnetism in non-annealed BPNMs is poor and some samples even show M_s values smaller than $\sim 0.3 \times 10^{-4}$ emu/100 μm^2 (inset of Fig. 2C). In the FMC-GNMs, the zigzag-type edge atomic structure is the most stable structure from both thermal and chemical perspectives[6,10-12], hence annealing at the T_c resulted in the formation of zigzag pore edges and the subsequent appearance of FM after H-termination. The occurrence of similar pore-edge atomic reconstruction to a zigzag is also expected for the pores of the present BPNMs (Fig. 1B) following annealing at the T_c, thus also leading to FM after O-termination (Fig. 2A). This can be confirmed by Raman spectroscopy in later part.

Figure 2D shows the magnetization curve for the BPNM obtained after annealing under an H_2 atmosphere at 300 °C for 2 h immediately after formation of the nanopores. In contrast to the O-terminated BPNM, it can be seen that the H-terminated BPNM barely exhibit a FMC-hysteresis loop. Moreover, the M_s of an O-terminated sample subsequently annealed under an H_2 atmosphere at $T_c \sim 300$ °C for 5 h (Fig. 2E) is ~ 3 times less than that of the original O-terminated sample (Fig.2A). The disappearance of FM in the H-terminated BPNM is consistent with the theoretical prediction of the disappearance of FM in PNRs with H-terminated zigzag edges[26]. In particular, the result in Fig. 2E suggests that O-termination of the zigzag pore edges is highly stable and cannot be entirely replaced by H-termination.

Temperature-dependence of M_s and magnetization close to residual magnetization (M_r) are shown in Fig. 2F (SM 8). Both M values monotonically increase with decreasing temperature (e.g., from $\sim 0.65 \times 10^{-4}$ emu/100 μm^2 (300K) to $\sim 1.0 \times 10^{-4}$ emu/100 μm^2 (2K) for H = 10 Oe and ~ 0.7 (300K) to ~ 1.2 (2K) for H = 200 Oe). Hence, the difference of M_s and M_r values between 2K and 300K is evident. This result definitely supports the presence of the FMC hysteresis loops at 2K and 300K in our O-terminated BPNMs.

Figure 3 shows the residual magnetization (M_r) of FMC-BPNMs (O-terminated BPNMs) as a function of the interpore distance (W), which is identical to the width of a PNR, and M_s as a function of the thickness (d) and sample area (S). The M_r value seems to be not very sensitive to W (Fig. 3A). This is controversial when compared to flat band FM in GNMs, there the Coulomb exchange interaction between opposite edges strongly decreases with W, leading to a loss of the stability of the FMC spin ordering and hence a lower M_r[15]. This is, however, consistent with previous theories of ZPNRs[17,21] and with our theoretical prediction described below.

On the other hand, the M_s values are linearly enhanced as d and S increases (Figs. 3B and 3C). In particular, the dependence on d suggests that M_s value of mono-layer BPNM becomes negligible. This is associated with strong interlayer interactions in AB stacking of BP (Fig. 1A), which favors the FMC spin configuration and analogous to graphene[19]. Our theoretical calculations for zigzag-PNR actually support this result and also indicate even much stronger interlayer interaction as explained in later part (Fig. 5E, 5F). This interlayer spin interaction makes long-range spin ordering stable even at 300 K (Fig. 2A). The linear dependence on S (Fig. 3C) arises because the area of the O-terminated zigzag pore edges linearly increases with increasing S. This means that the fully O-terminated pores uniformly exist through all layers in individual samples. This implies that the O-termination of the pore edges of BPNMs can be easily realized only by exposing samples to air atmosphere and significantly contributes to the observed large-magnitude edge magnetism.

As discussed above, annealing at T_c may cause the reconstruction of the pore-edge atomic structure, resulting in formation of zigzag pore edges and subsequent occurrence of FM after O-termination[26]. Evaluation of typical Raman spectra of BPNMs that did and did not exhibit FM evidently supports this argument (Fig. 4A). From Fig. 4A, it is confirmed that the heights of the band peaks due to the phonons resulting from interlayer interactions (I_{Ag1}) are nearly the same in the

spectra of the two samples, while the intensity of the band attributed to the phonon from the Si substrate (I_{Si}) is significantly larger in the non-FMC sample, leading to a low I_{Ag1}/I_{Si} value. We find that this tendency agrees with that confirmed for the bulk regions and edges of few-layer BP flakes (i.e., without nano-pores) of different d that were not annealed at T_c (Fig. 4B). Fig. 4B implies that the I_{Ag1}/I_{Si} ratios observed at the edges is lower than those of the corresponding bulk regions in nearly all of the samples (Inset), and an approximately linear correlation between the I_{Ag1}/I_{Si} ratio and d was obtained[16]. The lower I_{Ag1}/I_{Si} values at the edges can be obtained from the same relationship as that in Fig. 4A (i.e., the higher peak value of I_{Si}). Indeed, the I_{Ag1}/I_{Si} values for the FMC (○) and non-FMC (×) BPNMs, including those shown in Fig. 4A, follow the peak trends for the bulk regions and edges plotted in Fig. 4B, respectively.

The lower I_{Ag1}/I_{Si} values at the edges of BP flakes can be attributed to presence of the armchair-rich edges, while the I_{Ag1}/I_{Si} values ~ 1 in the bulk region suggests presence of zigzag-rich edges, from the following two reasons. First, because the BP flakes without nano-pores were just mechanically exfoliated from bulk BP without any intentional alignment of crystal axis and not by annealing at the T_c, the edge atomic structures should be rough edges but arm chair rich. This is because zigzag edge appears only when crystal axis is perfectly aligned along Y axis in Fig. 1A, while in any other cases the buckling armchair edge appears.

Second, the intensity of the phonons from the Si substrate at the armchair edges is higher than that of phonons at the zigzag edges, because the buckling armchair structures are formed along z-axis (Fig. 1A) and the surface of the Si substrate can easily oscillate under them (e.g., beneath gray P atoms) [20]. However, these effects are suppressed in bulk region in few layer BPs and, hence, the I_{Ag1}/I_{Si} values are not high. On the other hand, all phonons are induced more effectively in sample edges than at bulk regions, because the sample has a free end. This inducement is more significant for phonon arising from Si substrate under the arm chair structure from the abovementioned reasons. Hence the low I_{Ag1}/I_{Si} ratios arising from the high I_{Si} values detected at the edges (Fig. 2B) is attributed to the buckling armchair edge.

This behavior should be analogous to the behavior observed in the non-FMC and FMC BPNMs (Figs. 4A and 4B), because a BPNM is a large ensemble of BPNRs with edges (Fig. 1E). Hence, the low I_{Ag1}/I_{Si} ratios in Fig. 4A suggest the armchair-rich pore edges in the non-FMC BPNM. In contrast, it can be concluded that the pore edge of the FMC BPNMs is zigzag rich, which are formed by edge reconstruction during annealing at the T_c. This also suggests emergence of partial zigzag edges in other four pore edges in addition to the two zigzag pore edges (inset of Fig. 2A) (SM 7)[27].

To theoretically reconfirm the present edge-magnetism in O-terminated ZPNRs, we have carried out first principles calculations (SM 9). Figure 5A shows the band structure of the relaxed O-terminated 10-ZPNRs (Fig. 5B) considered in our calculations. The left and right panels correspond to the spin-unpolarized and -polarized cases, respectively. Similarly to previous calculations, a pair of midgap states (red arrow in Fig.5A) span across the band gap and cross the Fermi level at around $\pi/2a$ of the Brillouin zone (BZ) inducing a metallic state. The midgap states at Γ and X (right panel of Fig. 5A) are completely localized along the edges as seen in Figs.5B and 5C. This is related to the small band splitting observed at the Γ-point for O-terminated PNRs, which is much smaller than [25], and implies a strong reduction of inter-edge coupling in presence of O[28]. This is in agreement with Fig.3A.

The magnetic moments emerging at the O atoms couple ferromagnetically with the ones at the neighboring P$_{edge}$ atoms giving rise to a huge enhancement of the edge magnetism (the green arrows in Fig. 5C; SM 9). The values of the local magnetic moment M_L at the P$_{edge}$ and O atoms for the O-terminated 10-ZPNR are $|M_P|$ = 0.55 μ_B and $|M_O|$ = 0.4 μ_B, respectively (very similar to the O-terminated 6-ZPNR). The calculated total M_L is around 1 μ_B per P=O dimer, almost seven times bigger than those in [21]. We also reveal that at the X-point the spin densities from the valence bands are only localized along the edges of the NR which strongly contributes to the edge-Anti-FMC state (SM 9). Although the M_L value is only a few times larger than that of the FMC-GNMs (M_L ~ 0.2 or 0.3 μ_B), the uniform oxidation of pore edges through all layers in a BPNM allows this large magnetism. Since the H-termination eliminates the abovementioned unsaturated bond, magnetism disappears.

Behavior of interlayer edge-spin coupling in the O-terminated ZPNRs is shown in Fig. 5D (SM 9). Misalignment of interlayer adjacent O=P$_{edge}$ atoms in AB stacking allows FMC spin configuration in bilayer ZPNRs as well as the case of few-layer GNRs. However, the strong interlayer interaction due to the O atom (SM 9) induces this FMC spin alignment and makes spin ordering more stable. Indeed, the linear scaling of the absolute magnetization, defined as the sum of the absolute values of the M_L (m_i) on each atom, $|M| = \Sigma_i |m_i|$, is confirmed with the number of layers (N) as shown in Fig.5D. This is qualitatively consistent with Fig. 3B .

References and notes

1. Nakada, K., Fujita, M., Dresselhaus, G., and Dresselhaus, M. S., *Phys. Rev. B* **54,** 17954 (1996).
2. Soriano, D. *et al.*, *Phys. Rev. Lett.* **107**, 016602 (2011).
3. Lee, H. *et al.*, *Chem. Phys. Lett.* **398**, 207 (2004).
4. Kusakabe, K. and Maruyama, M., *Phys. Rev. B* **67**, 092406 (2003).
5. Shimizu, T., Haruyama, J. *et al.*, *Nature Nanotech.* **6,** 45 (2011).
6. Tada, K., Haruyama, J., Chshiev, M. *et al, Phys. Status Solidi B* **249**, 2491 (2012). In GNM, *H*-terminated zigzag edges yielded flat-band FM, while *O*-terminated edges exhibited diamagnetism.
7. Kato, T., Nakamura, T., Haruyama, J. *et al.*, *Appl. Phys. Lett.* **104**, 252410 (2014).
8. Hashimoto, T., Haruyama, J., Soriano, D., Roche, S. *et al.*, *Appl. Phys. Lett.* **105**, 183111 (2014).
9. Hashimoto, T., Haruyama, J. *et al., Mat. Sciences and Appl.* **5(1)**, 1 (2014).
10. Jia, X., Dresselhaus, M. S. *et al., Science* **323**, 1701 (2009).
11. Girit , C. O. *et al., Science* **323**, 1705 (2009).
12. You, Y., Ni, Z., Yu, T. and Shen, Z. *Appl. Phys. Lett.* **93,** 163112 (2008).
13. Li, L. *et al., Nature Nanotech.* **9**, 372 (2014).
14. Herrero, P.-J. *et al., Nature Nanotech.* **9**, 330 (2014).
15. Koenig, S. P. *et al., Appl. Phys. Lett.* **104**, 103106 (2014).
16. Gomez, A. C. *et al., 2D Materials* **1**, 025001 (2014).
17. Zhu, Z. *et al., Appl. Phys. Lett.* **105**, 113105 (2014). Non-fully relaxed structure was assumed in order to avoid Peierls transition. This predicted local edge magnetic moments M_L of 0.27 μ_B for the O atom, 0.39 μ_B for the edge P atom, and 0.13 μ_B for its nearest neighbor, respectively.
18. Peng, X. *et al., J. Appl. Phys.* **116**, 144301 (2014).
19. Carvalho, A., Rodin, A. S., and Neto, A. H. C., *Euro. Phys. Lett.* **108**, 47005 (2014).
20. Ong, Z. Y., Cai, Y., Zhang, G., Zhang, Y. –W., arXiv:1409.097. The phonon dispersion along the zigzag direction was shown to be sharper than that along the armchair direction using first-principles calculations for BP.
21. Du, Y. *et al.*, *Sci. Rep.* **5**, 8921 (2015). The half-filled 1D bands crossed the Fermi level at around $\pi/2a$ for ZPNRs, showing emergence of no Peierls transition. This with edge-AFMC ordering reported 0.155 μ_B for the edge P.
22. Zhu, W. *et al.*, *Nano Lett.* **15**, 1883 (2015).
23. Ziletti, A., Neto, A. H. C. *et al.*, *Phys. Rev. B* **91**, 085407 (2015). Oxidation resulted in O-termination of the pore edges, because oxidized top layers serve as protection layers of underneath BP layers preventing their bulk oxidation
24. Dai, J. and Zeng, X. C., *J. Phys. Chem. Lett.* **5**, 1289 (2014).
25. Luo, X., Lu, X., *et al.*, *Nano Letters* **15**, 3931 (2015).
26. Because the BPNM tends to disappear when annealing at T > 350 °C, the annealing temperature of 300 °C is approximately the T_c, at which the reconstruction of pore-edge atomic structures occurs in the BPNMs. This T_c is much lower than ~800 °C for the FMC-GNMs.
27. Only two out of ten BPNMs did not result in zigzag-rich pore edges after annealing at the T_c, thus did not exhibit FM due to this armchair-rich edge (SM 7). It also suggests that the buckling armchair edge requires higher energy for stability after the T_c annealing and is hard to be realized. The reconstruction by the T_c annealing may introduce relaxed structure to interpore BPNRs, which conventionally results in Peierls transition and disappearance of magnetism[18, 21]. However, the present BPNM structure, in which six BPNRs with a typical width ~20nm form one hexagonal unit cell leaving a nano pore at the center, may prevent occurrence of Peierls transition.
28. We have also checked inter-edge magnetic coupling for both parallel and antiparallel couplings of edge-FMC and edge-Anti-FMC (AFMC) configurations in the doubly relaxed unit cells. We found that the total energies were very similar ($\Delta E < 1$ meV), which highlights the small spin interaction between edges. The edge-FMC configuration with antiparallel inter-edge coupling (similar to zigzag GNRs) always led to non -magnetic or bad converged solutions. In contrast, the edge-AFMC configuration always converged very fast while keeping the initial AFMC guess along the edge. Interestingly, the O atoms were not initially polarized and became magnetic during the self-consistency calculation.
29. (1) The total area of typical few-layer bulk BP flakes used for the nanomesh formation is $\sim 10^3$ μm^2. (2) The area of one hexagonal unit cell with a pore is S = $6(3^{-1/2}/2)(a/2)^2$ ~4300 nm^2, where a = [80 nm (pore diameter) + 20 nm (pore spacing)]. (3) Thus, the total number of holes is $(\sim 10^3$ $\mu m^2 \times 10$ layers)/ (4300 nm^2) ~2.5 $\times 10^6$ [i.e., (1)/(2)]. (4) The saturation magnetization per a single pore area is thus estimated to be ~1.2×10^{-3} (emu) $\times 10^{-3}/$~2.5 $\times 10^6 =$ ~0.5×10^{-12} (J/T).
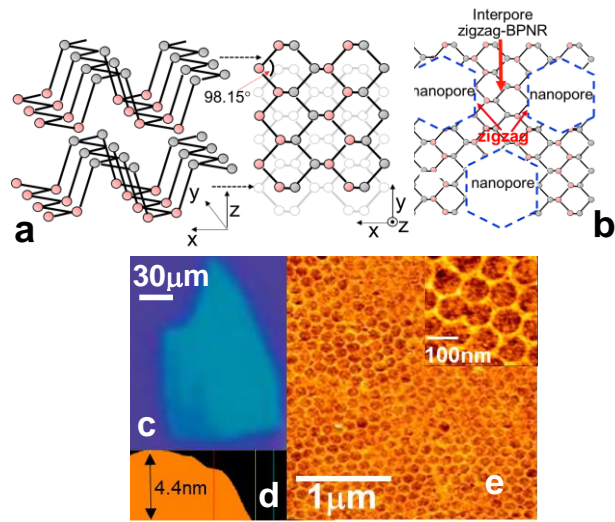
Fig. 1
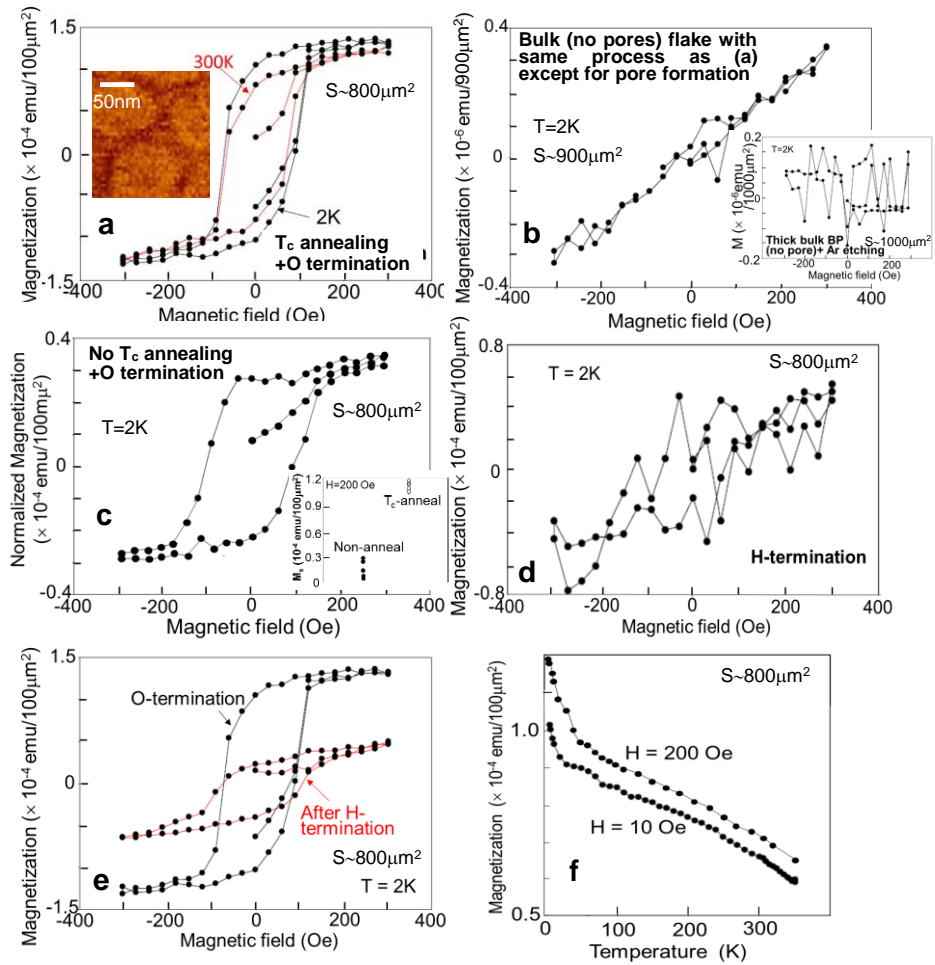
Fig. 2

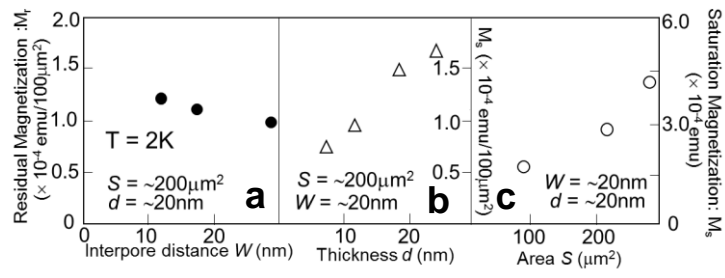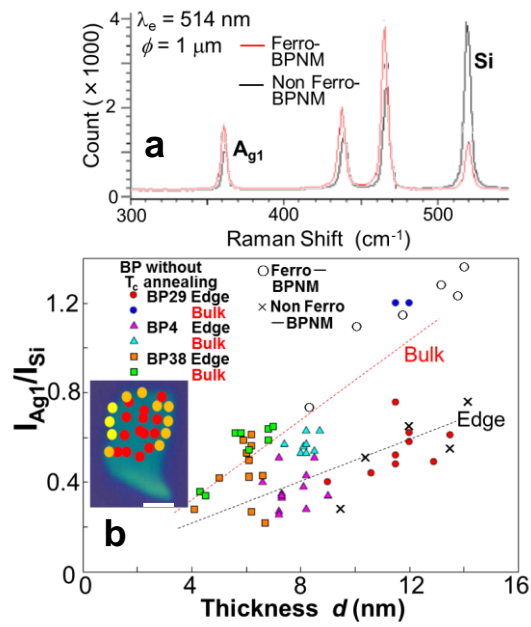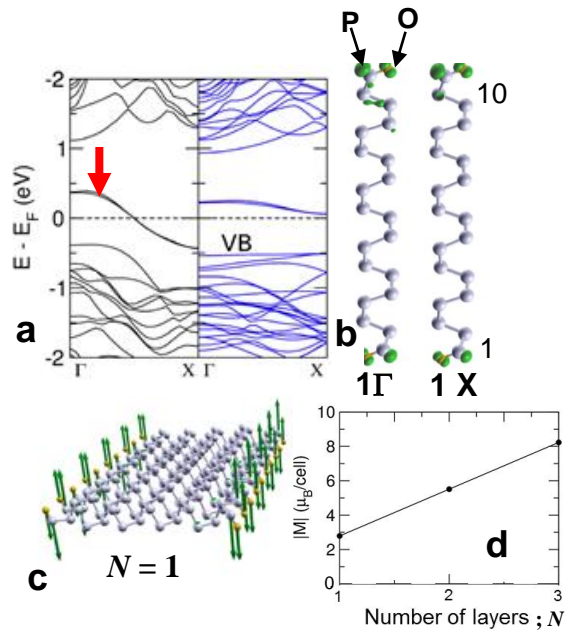**Fig. 3**

Fig. 4

Fig. 5

Figure captions

Fig. 1 **(a)** Schematic cross-sectional and top views of a puckered honeycomb lattice of two-layer black phosphorens with AB stacking. Gray and red symbol's P atoms locate within different height. Zigzag edge is within mono layer along y axis, while buckling arm chair edge is formed to z-axis direction along x axis. **(b)** Schematic top view of a BPNM, in which two pore edges are perfectly aligned to zigzag structure. In actual structure, pore size and interpore spacing are much larger and larger number of P atoms exists at the interpore BPNR regions. **(c)** Optical microscope image of a flake of few-layer BP mechanically exfoliated from bulk BP. **(d)** Cross-sectional image of (c) obtained using atomic-force microscope. **(e)** Atomic-force microscope top-view image of a BPNM with a large number ($\sim 10^{11}$) of pores, which was fabricated via. non-lithographic method (SM1-5) in an extremely careful way (e.g., using plastic tweezers) to avoid incorporating magnetic impurities, magnetic defects, and magnetic contamination. **Inset:** Higher magnification image.

Fig. 2 **(a, c-e),** Magnetization curves for BPNMs with **(a)** T_c annealing and O-termination, **(c)** no T_c annealing and O-termination, **(d)** H-termination, **(e)** H-termination of the sample in (a). **Inset of (a),** Observation of (a)-sample by magnetic force microscope under H = 10 Oe at T = 300K. Darker parts mean higher density of polarized spins. **Inset of (c),** Saturation magnetization (M_s) of T_c- and no T_c-annealed BPNMs (each five samples) BPNMs at 2K. **(b)** Magnetization curve for few-layer bulk BP flake (i.e., without nano pores) through all the same fabrication process as those for (a)-sample except for the pore formation. **Inset of (b)**; Magnetization for bulk thick BP (with no pores) with Ar gas etching process without using porous alumina template mask (but with the same condition as that for pore forming). For all samples, no background magnetism was subtracted except for (c), in which a diamagnetic background line was subtracted. S is the sample area including the total pore area. Results of Fig. 2(b) are independent of S. **(f)** Temperature dependence of magnetization values of a magnetic BPNM (i.e., with T_c annealing and O-termination) measured with decreasing temperatures.

Fig. 3 **(a)** Residual magnetization (M_r) of FM BPNMs as a function of the interpore distance (W) (i.e., width of the interpore PNR regions), and M_s as a function of the **(b)** thickness (d) and **(c)** sample area (S).

Fig. 4 **(a)** Typical micro Raman spectra for two BPNMs that do and do not exhibit ferromagnetism. **(b)** Correlation of the d and I_{Ag1}/I_{Si} values in the Raman spectra measured in the bulk and at the edges of three few-layer BP flakes (i.e., without nanopores) without T_c annealing. The linear dotted lines indicate trends for the individual correlations. The I_{Ag1}/I_{Si} values for the FM (◯) and non FM (✕) BPNMs, including the result of Fig. 4(a), are also noted. **Inset:** Example of Raman mapping for sample BP4 in main panel. Red, orange, and yellow symbols mean the measured points with results of $I_{Ag1}/I_{Si} > 0.5$, $0.5 > I_{Ag1}/I_{Si} > 0.3$, $0.3 > I_{Ag1}/I_{Si}$, respectively.

Fig. 5 **(a)** Band structures for O-terminated 10-ZPNR. Left and right panels correspond to spin-unpolarized and -polarized cases (SM9). **(b)** Charge density contribution (shown in green) of one of the midgap states (red arrow in (a)) at Γ and X. The structure corresponds to O-terminated interpore ZPNR region of BPNM. Distances are very similar to those reported for mono-layer PNR. The distance between P and O atoms at the edges is 1.5 Å, which corresponds to a P=0 double bond. **(c)** Illustration of the edge anti-FM emerging at the zigzag edges of (b). Green arrows correspond to the spin magnetic moment computed on each atom. **(d)** Scaling of the absolute magnetization per unit cell with number of layers (N). Relaxed interlayer-distance ($d_z \approx 0.198$ nm) is around 0.1 nm shorter than previously report.